American Journal of Pathology, Vol. 146, No. 6, June 1995

Dynamics of Cell Proliferation and Cell Death during the Emergence of Primitive Neuroectodermal Tumors of the Immature Central Nervous System in Transgenic Mice

Kar-Ming Fung, Virginia M.-Y. Lee, and John Q. Trojanowski

From the Department of Pathology and Laboratory Medicine, Division of Anatomic Pathology, Division of Neuropathology, Hospital of the University of Pennsylvania, Philadelphia, Pennsylvania

Cell proliferation and cell death play critical roles in embryonic development, postnatal tissue maintenance, and tumor formation. To understand the interplay between cell proliferation and death in tumor formation, we studied these two processes in nascent primitive neuroectodermal tumors that arose postnatally from neuroepithelial cells ventral to the median eminence of transgenic mice (designated rTH-Tag mice) carrying a Simian virus 40 large T antigen transgene driven by a rat tyrosine hydroxylase promoter. Cell proliferation continued in the neuroepithelium of the ventral median eminence in wild-type and transgenic animals for the first 2 weeks of postnatal life but subsided completely in the wild-type mice after 2 weeks of age. In contrast, mitotic activity persisted in these progenitor cells of the rTH-Tag mice, and there was a dramatic increase in mitotic activity after 10 weeks leading to the formation of primitive neuroectodermal tumors despite sustained cell death activity. We conclude that primitive neuroectodermal tumors originate from progenitor cells in the ventral median eminence of rTH-Tag mice in early postnatal life when progenitors fail to respond to signals to exit the cell cycle. Thus, the disruption of mechanisms that regulate cell proliferation and cell death in the developing brain may underlie the emergence of primitive neuroectodermal tumors in the rTH-Tag mice. (Am J Pathol 1995, 146:1376–1387)

The total number of cells in a population is maintained constant only if cell proliferation equals cell loss. At least two major modes of cell death have been identified, ie, necrosis and apoptosis. Necrosis, the end product of cell injury, is seen in tumors and many other pathological conditions but not in normal cells or tissues. On the other hand, programmed cell death or apoptosis[1,2] occurs in normal physiological processes such as tissue remodeling in embryogenesis[3] and in the homeostasis of cell populations[4] as well as in pathological processes.[5–7] Unlike necrosis, apoptosis is an active form of cell death that appears to be genetically controlled.[8–11] Furthermore, in some cases apoptosis also appears to be dependent on the cell cycle status.[12] Cells undergoing apoptosis display characteristic morphological and biochemical features such as condensed chromatin, apoptotic bodies, and fragmentation of genomic DNA at 185- to 200-bp intervals.[2,5,9,10,13]

Primitive neuroectodermal tumors (PNETs) are common pediatric brain tumors, and the cerebellar medulloblastoma is the prototype of this class of neoplasm.[14–18] Although PNETs exhibit the phenotypic properties of central nervous system (CNS) stem cells or neuronal progenitors,[14,18–20] current understanding of the mechanisms of tumorigenesis in the immature CNS and of the events leading to tumorigenesis and tumor progression in the developing human nervous system are almost completely unknown. However, recently developed animal models of PNETs provide an opportunity to explore these issues.[17,18,21] For example, studies of PNETs in several lines of mice that harbored a Simian virus 40 large T antigen (SV40-Tag) transgene showed that brain tu-

Supported in part by grants (CA-16520 and CA-36245) from the National Cancer Institute.

Accepted for publication March 1, 1995.

Address reprint requests to Dr. John Q. Trojanowski, Department of Pathology and Laboratory Medicine, Division of Anatomic Pathology, The University of Pennsylvania School of Medicine, HUP/Maloney Basement, Room A009, 3600 Spruce St., Philadelphia, PA 19104-4283.

mors arising in these mice are phenotypically similar to human undifferentiated PNETs or PNETs with a neuronal phenotype.[21] Indeed, PNETs arising in the SV40-Tag transgenic line driven by a rat tyrosine hydroxylase (TH) promoter (designated rTH-Tag mice) are nearly indistinguishable from human PNETs with neuronal differentiation.[21,22] Thus, these transgenic mice enable the investigation of early events leading to the formation of PNETs in the mouse CNS that are impossible to analyze in humans.

Tumorigenesis is a step-wise process involving the activation of oncogenes and/or the loss of tumor suppressor genes.[23] The salient feature of neoplastic transformation is the uncontrolled net increase in the total number of cells.[24] Thus, disruption of the balance between cell proliferation and death is a critical turning point in the emergence of a neoplasm. In many cases, the expression of SV40-Tag or other oncogenes *in vivo* results in uncontrolled cell proliferation leading to tumor formation in transgenic mice.[25] Paradoxically, SV40-Tag also may induce neuronal degeneration in some lines of transgenic mice without tumor formation,[26,27] or neoplastic transformation and neuronal degeneration may occur in the same population of cells that express SV40-Tag in other lines of transgenic mice.[28,29] However, the *in vivo* expression of SV40-Tag in transgenic mice may not result in any phenotypic manifestations.[21,22,30] These paradoxical observations are difficult to explain, but they suggest a linkage between mechanisms that regulate cell proliferation and cell death during tumor formation. In addition, the genetic and the epigenetic events that control these processes may be cell type specific.[8,10,31]

To probe the role of cell proliferation and death in PNETs induced by SV40-Tag, we dissected the earliest cellular events in the genesis of PNETs in the rTH-Tag transgenic mice by studying these mice at different postnatal ages. Cell proliferation in these PNETs and the neuroepithelium in which they arose was studied by *in vivo* bromodeoxyuridine (BrdU) labeling,[32] and cell death was monitored by the terminal deoxynucleotidyl transferase-mediated biotinylated dUTP nick end labeling (TUNEL) technique *in situ*[33] by light and electron microscopy as well as DNA gel electrophoresis.[13] On the basis of these studies, we conclude that the transition from a preneoplastic state to an overt PNET is heralded by an aberrant surge in proliferative activity that perturbs the balance between cell proliferation and cell death in a population of neuroepithelial cells that fail to regress normally in the median eminence of postnatal rTH-Tag mice.

Materials and Methods

Transgenic and Wild-Type Mice

The studies described here were conducted on rTH-Tag transgenic mice[22] from 1 week to >20 weeks of age. The presence of the transgene was screened by Southern blot technique, and littermates carrying no transgene were used as controls. These studies were performed according to protocols approved by the Committee on Studies Involving Animals of the University of Pennsylvania.

Southern Blot Analysis

DNA was extracted from tissue by proteinase K digestion followed by phenol-chloroform extraction and ethanol precipitation. After restriction enzyme digestion (*Bam*H1) and separation by electrophoresis in 1% agarose gels, DNA was affixed to Zeta-Probe membranes (Bio-Rad, Richmond, CA) by capillary transfer followed by ultraviolet cross-linking. The membranes were prehybridized in Quick-Hyb solution (Stratagene, La Jolla, CA) followed by hybridization with an [α^{32}P]dCTP-labeled DNA probe synthesized (Prime-It II kit, Stratagene) from a SV40-Tag-specific template.[34] The membranes were washed according to the vendor's instructions and exposed to x-ray film at −70 C for 2 to 4 days before development.

BrdU Labeling

Animals were pulsed with five injections of BrdU at 2-hour intervals (50 μg/g body weight/injection) as described.[32] Mice were sacrificed between 30 to 120 minutes after the last injection by CO_2 asphyxiation, and they were perfused by phosphate-buffered saline followed by 4% paraformaldehyde in phosphate-buffered saline. The brains were post-fixed in the same fixative overnight before being processed into paraffin blocks. Serial sections were cut at 6 μ, affixed to slides, and stored at room temperature until further use. The proximal jejunum was routinely examined as a control to evaluate the efficiency of BrdU labeling.

Immunohistochemistry

Sections were evaluated initially by hematoxylin and eosin staining to identify the PNETs followed by immunohistochemistry with a panel of well characterized antibodies against neural and other antigens including the low molecular weight neurofilament protein (NF-L), nestin, neural cell adhesion molecules

(N-CAM), SV40-Tag, synaptophysin, TH, and BrdU (Table 1). Sections were stained by the peroxidase-antiperoxidase technique or the avidin-biotin complex technique with streptavidin conjugated to either peroxidase (GIBCO BRL, Gaithersburg, MD) or alkaline phosphatase (BioGenex, San Ramon, CA). Microwave enhancement was performed as previously described.[40,41] In single primary antibody staining experiments, the peroxidase system was used and developed in diaminobenzidine (DAB) with hydrogen peroxide as described,[40,41] and the sections were counterstained with hematoxylin, dehydrated, cleared, and mounted in an organic based medium. In double primary antibody staining experiments to demonstrate BrdU-labeled nuclei and a cytoplasmic or cell surface antigen, the incorporated BrdU was visualized by the peroxidase-antiperoxidase technique with DAB, and the cytoplasmic or cell surface antigen was visualized by the avidin-biotin complex-alkaline phosphatase technique with fast red (1 mg/ml; Sigma Chemical Co., St. Louis, MO) with AS-MX naphthol phosphate buffer (0.4 mg/ml in 0.1 mol/L Tris, pH 8.2; Sigma) and 0.6 mg/ml levamisole (Sigma) for 15 minutes. These sections were counterstained with hematoxylin and mounted in an aqueous based medium.

TUNEL Staining

The TUNEL method was performed as described.[33] Briefly, deparaffinized and rehydrated slides were digested with 20 μg/ml proteinase K in 0.1 mol/L Tris, pH 8, at room temperature for 15 minutes. After washing, the sections were incubated with a mixture containing 20 mmol/L biotinylated dUTP, 0.3 U/μl terminal deoxynucleotidyl transferase, 1.5 mmol/L cobalt chloride, 200 mmol/L sodium cacodylate, 25 mmol/L Tris, and 0.25 mg/ml bovine serum albumin, pH 6.6, at 37 C for 45 minutes. The reaction was terminated by washing in 2X standard saline citrate (0.3 mol/L sodium chloride, 0.03 mol/L sodium citrate) for 15 minutes, and the results were visualized by alkaline phosphatase-conjugated streptavidin and developed as described above. Coronal sections of a postnatal day 8 rat brain were used as positive controls because apoptotic activity peaks in neocortex at this age.[3]

Table 1. *Antibodies Used in This Study and Their Specificity*

Specificity	References
Rabbit polyclonal antibodies	
NF-L	20, 21
Nestin	20, 21
N-CAM	21, 35
SV40-Tag	21, 36
Mouse monoclonal antibodies	
Synaptophysin (clone SY38)*	21, 37
Tyrosine hydroxylase (clone MR 3)*	38
BrdU (clone BU-33)†	39

*Purchased from Boehringer Mannheim (Indianapolis, IN).
†Purchased from Sigma Chemical Co. (St. Louis, MO).

Electron Microscopy

To examine the ultrastructure of TUNEL-positive cells, TUNEL staining was performed with peroxidase-conjugated streptavidin and developed in DAB as described above. A solution of 3% hydrogen peroxide in methanol was applied for 5 minutes at room temperature before the proteinase K digestion step to block endogenous peroxidase activity. After the DAB reaction, the sections were first treated with 0.1 mol/L cacodylate buffer and then post-fixed in 4% osmium tetroxide for 10 minutes at room temperature. They were then dehydrated with graded alcohols and embedded *in situ* in Polybed 812 resin (Polyscience, Warrington, PA). Thin sections were cut, collected on nickel grids, stained with lead citrate, and examined under a Hitachi H-600 electron microscope at 75 kV.

Quantitation of Cell Proliferation and Cell Death

The BrdU and the TUNEL labeling index of a sample was defined as the number of positively stained cells divided by the total number of cells in the same microscopic field viewed with a ×40 objective. For each mouse, the number of positively and negatively labeled cells was determined in approximately 500 to 1500 cells in randomly selected microscopic fields of BrdU and TUNEL preparations.

Detection of DNA Fragmentation by Gel Electrophoresis

Fragmentation of genomic DNA was demonstrated by an autoradiographic method[13] with minor modifications. Notably, this method introduces only one molecule of [α-^{32}P]ddATP at the 3′ end, and this has negligible effects on the molecular weight of the DNA fragments. Tumor tissue and control mouse cerebellum were snap frozen in liquid nitrogen and stored at −70 C before use. Briefly, tissue fragments were homogenized and incubated at 68 C for 1 hour in homogenizing buffer (0.1 mol/L NaCl, 0.01 mol/L EDTA, 0.3 mol/L Tris-HCl, 0.2 mol/L sucrose, 0.6% sodium

dodecyl sulfate, pH 8.0). Then, 8 mol/L potassium acetate was added to a final concentration of 1.15 mol/L followed by incubation on ice for 1 hour. Protein precipitates were spun down in a microfuge at 14,000 rpm for 30 minutes at 4 C. The supernatants were removed and digested with DNAse-free RNAse at a final concentration of 2 μg/ml at 37 C for 1 hour. The samples were then extracted with an equal volume of phenol/chloroform/isoamyl alcohol followed by an equal volume of chloroform/isoamyl alcohol. DNA was precipitated with an equal volume of isopropanol at −70 C for 5 minutes and then at −20 C for at least 1 hour. The DNA was spun down in a microfuge at 14,000 rpm for 30 minutes at 4 C and washed with ice-cold 70% ethanol twice followed by drying in a Speed-Vac concentrator (Savant Instruments, Farmingdale, NY). The pellets were dissolved in 50 μl of sterile distilled water, quantitated by absorbance at 260 nm and stored at −20 C before use.

For each 3′ end labeling reaction, 1 μg of sample DNA was incubated with 30 U of terminal deoxynucleotidyl transferase (GIBCO BRL), 10 μl of 5X concentrated reaction buffer (GIBCO BRL), 30 μCi of [α-^{32}P]-ddATP (Amersham, Arlington Heights, IL), and water in a final volume of 50 μl at 37 C for 1 hour. The reaction was terminated by adding 2.5 μl of 0.5 mol/L EDTA. Labeled DNA was precipitated by adding 0.2 volume of 10 mol/L ammonium acetate, 50 μg of yeast tRNA (Sigma), and 3 volumes of ice-cold ethanol followed by precipitation for 1 hour at −70 C. The DNA pellets were collected as described above and resuspended in 50 μl of TE buffer (10 mmol/L Tris, 1 mmol/L EDTA, pH 8.0). They were precipitated the second time to remove unincorporated nucleotides. The pellets were then collected, dried, and dissolved in 20 to 40 μl of TE buffer followed by separation in 2% agarose gel in TAE buffer (40 mmol/L Tris-acetate, 1 mmol/L EDTA) as running buffer at a 10 V/cm length of the gel. After electrophoresis, the gel was soaked in 1.5 mol/L NaCl/0.5 mol/L NaCl for 30 minutes followed by 1.5 mol/L NaCl/1.0 mol/L Tris at pH 7.0 for 30 minutes. The DNA was then affixed to a Zeta-Probe membrane (Bio-Rad) by capillary transfer overnight. The membrane was then dried, sealed in a plastic bag, and exposed to x-ray film at −70 C for 2 to 6 hours before development.

Results

Site of Origin of PNETs

We located the site at which the PNETs originated by studying serial coronal and saggital sections of the transgenic mice. In all mice carrying SV40-Tag, microscopic lesions characterized by densely packed small blue cells could be demonstrated (Figure 1, A and B) within the median eminence ventral to the palisade zone. These cells were found in transgenic animals as young as 1 week old. In the age-matched postnatal control animals, a smaller and less extensive population of cells could be identified at the same location in young animals for as long as 2 weeks postnatal, but these cells were reduced to a thin layer permeated by a fine capillary network beyond 2 weeks postnatal (Figure 1, C to E). The regression of the neuroepithelial cells within the first 2 weeks of postnatal life has been observed previously.[42,43]

There was no substantial increase in the size of the population of neuroepithelial cells ventral to the median eminence in the transgenic animals from 1 week to 10 weeks of age. However, after a latent period of approximately 10 weeks, the preneoplastic lesions in the ventral median eminence of the rTH-Tag mice had progressed to form microscopic PNETs of variable dimensions. For example, in one litter of transgenic animals at 12 weeks of age, these cell populations appeared hyperplastic in only one mouse (Figure 1, F and H) whereas in another mouse they were clearly neoplastic (Figure 1G).

Cell Proliferation in PNETs

We quantitated the cell proliferation rate of nascent and established PNETs by using the *in vivo* BrdU method that labels cells in S phase. The length of the complete cell cycle minus the length of the S phase represents the theoretical shortest time that all cells in the cycle can be labeled by BrdU.[32] Although the exact length of the cell cycle of the PNET cells is unknown, and several clones of PNET cells with different cell cycle lengths might exist simultaneously, we used five pulses of BrdU at 2-hour intervals to label most cycling cells in the developing CNS.[44] This protocol enabled us to demonstrate BrdU labeling in PNETs at various stages in their induction and progression as well as in the progenitor cells that persist in the neuroepithelium of the ventral median eminence in transgenic mice (Figures 2, A and B, and 3) and in the wild-type mice (Figure 3).

A peak BrdU labeling rate of approximately 10% (Figure 3A) could be demonstrated in the densely packed neuroepithelial cells in the ventral median eminence of wild-type and transgenic mice less than 2 weeks old. In the control animals, the BrdU labeling rate decreased dramatically in the second week and

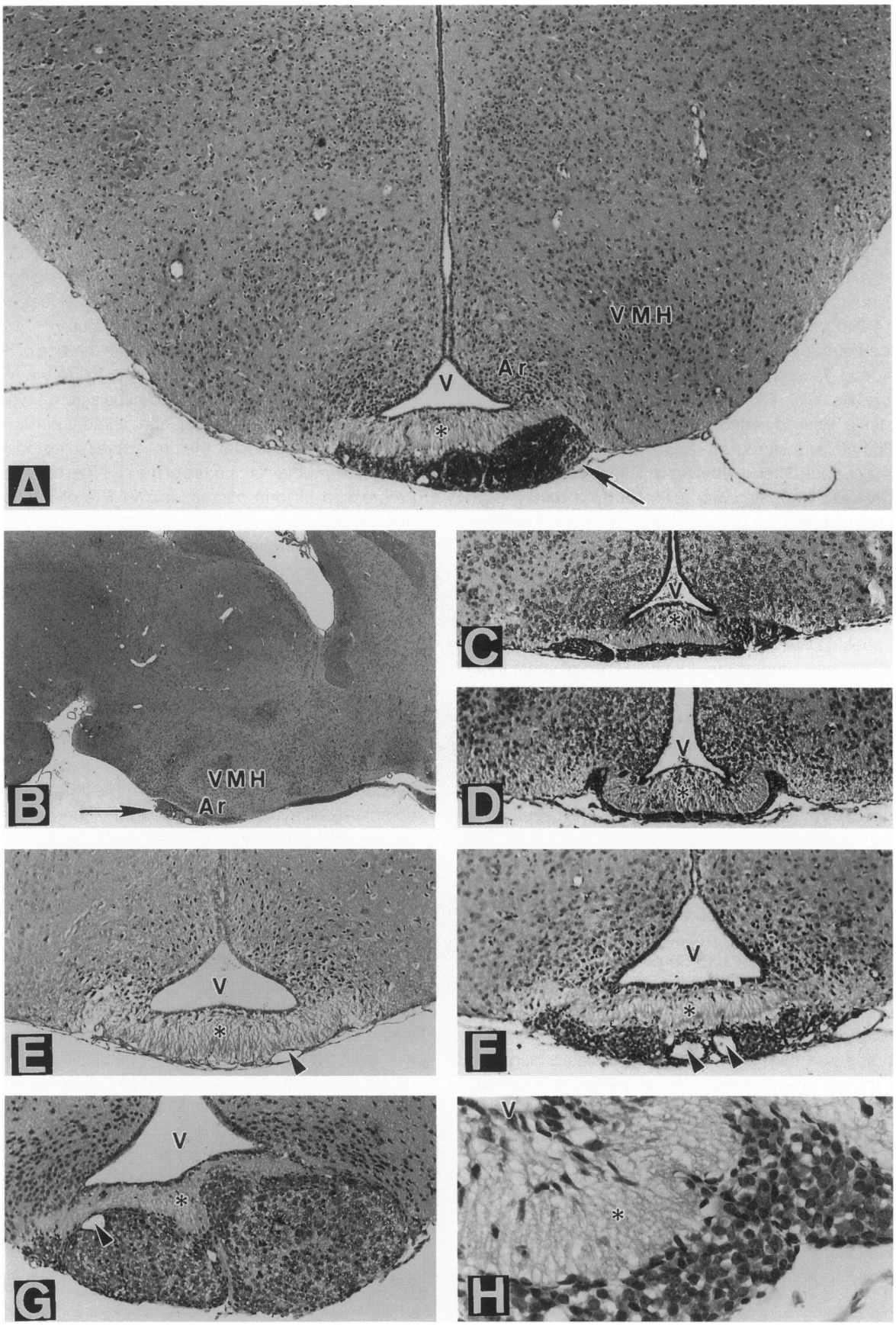
A
VMH
Ar
V
*
B
VMH
Ar
C
V
*
D
V
*
E
V
*
F
V
*
G
V
*
H
V
*

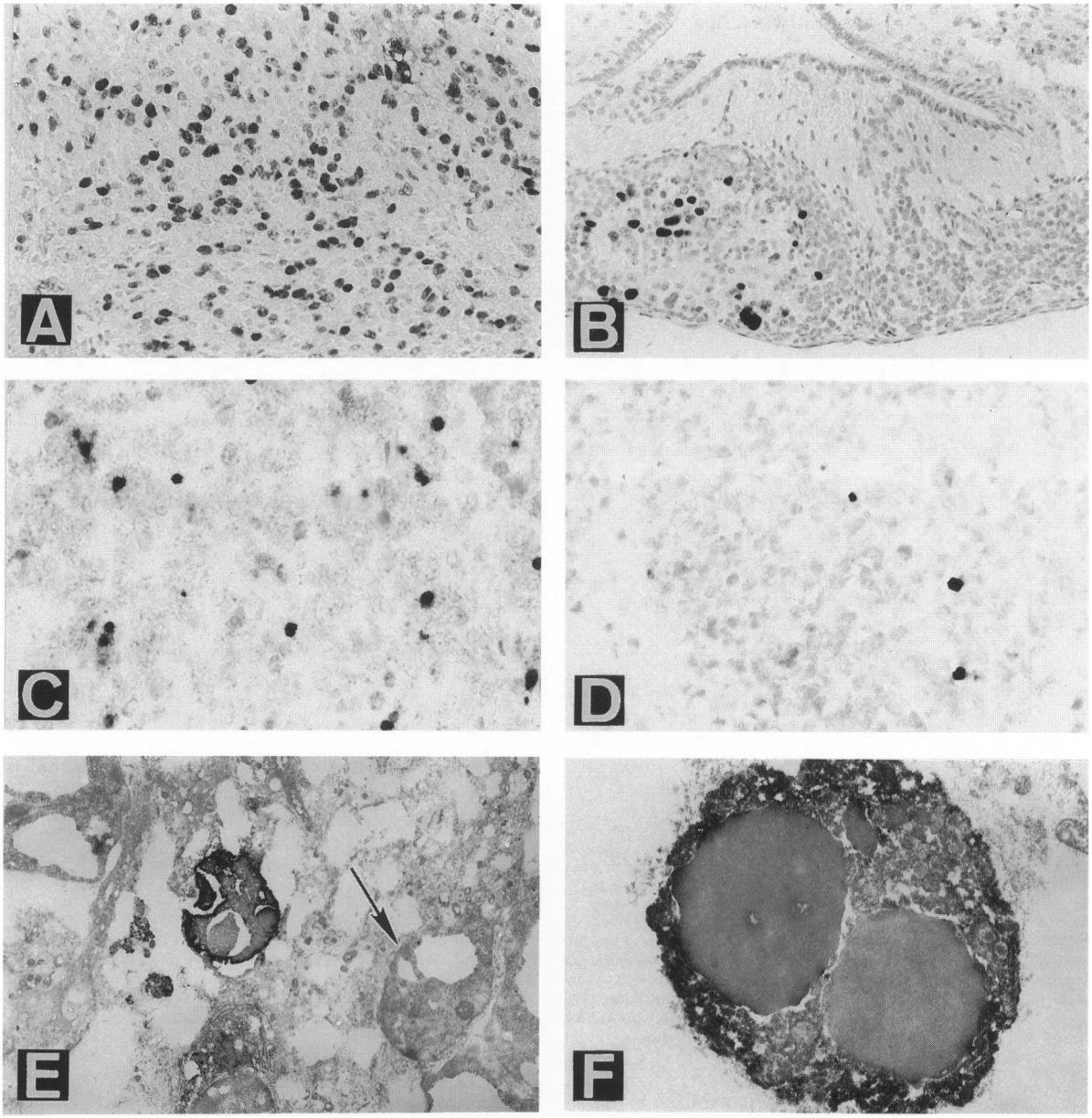

Figure 2. *Diffuse BrdU labeling can be demonstrated in advanced PNETs* (**A**), *whereas focal labeling is seen in nascent PNETs* (**B**). *A high* (**C**) *and low* (**D**) *abundance of TUNEL-positive cells can be demonstrated in different PNETs. At the ultrastructural level, TUNEL labeling is seen in the cytoplasm and the nucleus* (**E** *and* **F**). *Condensed chromatin typical of apoptotic cells is also seen. An unlabeled tumor cell without condensed chromatin also is seen (arrow in* **E**). (**A** *and* **B**, ×*160;* **C** *and* **D**, ×*320;* **E**, ×*3000;* **F**, ×*10000*)

remained zero in animals older than 4 weeks (Figure 3A, inset). The BrdU labeling rate in the transgenic mice also decreased nearly to zero in animals older than 2 weeks (Figure 3A), and the labeling rate remained very low until the animals were approximately 8 weeks old. However, in some 10-week-old transgenics, there was an abrupt surge in the BrdU labeling rate, and, in the older transgenics, the number of mice with a high labeling rate increased progressively as a function of age. The peak labeling rate in the

Figure 1. *Sections of nascent and established PNETs in transgenic mice stained with hematoxylin and eosin. Microscopic PNETs can be identified in transgenic mice in the ventral portion of median eminence* (*) *in coronal (arrow in* **A**) *and parasaggital sections (arrow in* **B**) *close to the arcuate nucleus (Ar in* **A** *and* **B**) *and the ventral medial hypothalamic nucleus (VMH in* **A** *and* **B**). *In 1-week-old mice, a layer of densely packed small blue cells can be seen in both the transgenic* (**C**) *and wild-type animals* (**D**). *This layer of cells completely regresses in adult wild-type mice* (**E**), *but they persist in the transgenic animals and continue to enlarge, albeit at different rates, to become tumors as shown in the two different 3-month-old transgenic mice* (**F** *and* **G**). *The arrowheads in* (**E**) *and* (**F**) *identify capillaries of the primary portal plexus. The cytological characteristics of these nascent PNETs are shown in* (**H**). *V, third ventricle.* (**A**, ×*55;* **B**, ×*16;* **C** *to* **G**, ×*80;* **H**, ×*320*)

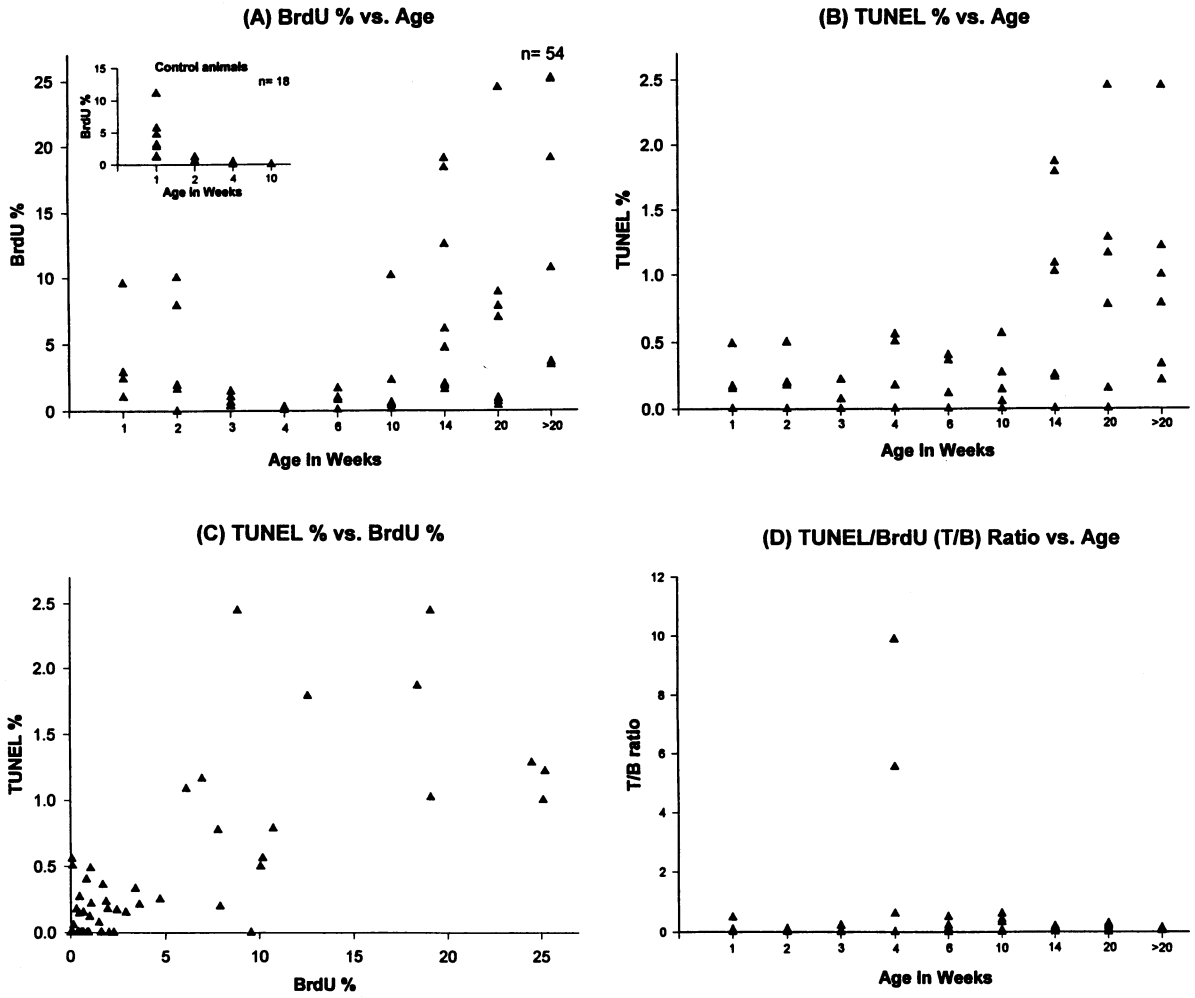

Figure 3. *This figure summarizes the quantitative analyses of cell proliferation and cell death in nascent and established PNETs in the rTH-Tag mice as well as in the neuroepithelium of the ventral median eminence of the wild-type mice. Each triangle represents one animal.* A: *Relationship between the BrdU labeling rate (BrdU %) and age. The inset in* (A) *shows the results obtained from the ventral median eminence in age-matched wild-type mice.* B: *Relationship between the TUNEL labeling rate (TUNEL %) and age. There was no TUNEL labeling in the neuroepithelium of the ventral median eminence of any of the wild type.* C: *Relationship between the BrdU and TUNEL labeling rates.* D: *Relationship of the TUNEL/BrdU ratio (T/B ratio) and age. See Results for a detailed discussion.*

transgenic mice rose to a maximum of 24.5% in mice older than 20 weeks (Figure 3A). We regarded the transition of low to high proliferation rate after the latent period as evidence of the transition from the preneoplastic to the neoplastic stage of PNET formation.

Cell Death in PNETs

TUNEL labeling enabled us to detect dying tumor cells in PNETs (Figure 2, C to F), but no TUNEL-positive cells were seen in neuroepithelium of the ventral median eminence in any of the wild-type mice. Characteristically, the TUNEL-positive cells were shrunken and scattered individually within a population of normal looking neuroepithelial cells in the young transgenic mice (Figure 2, C and D). Overt necrosis was seen only focally in advanced PNETs of macroscopic size. However, some TUNEL-positive cells were seen in the necrotic areas, but they were not included in the quantitative studies.

At the ultrastructural level, condensed chromatin characteristic of cells undergoing programmed cell death was evident in the TUNEL-positive cells (Figure 2, E and F). There was significant TUNEL labeling in the cytoplasm as well as in the nucleus. The cytoplasmic labeling may reflect the leakage of small 185- to 200-bp DNA fragments from the nucleus into the cytoplasm during apoptosis as described previously.[45] Gel electrophoresis of 3′ end radioactively labeled DNA purified from PNETs demonstrated DNA fragments at 185-bp intervals (Figure 4, lane B). This laddering pattern was not seen in

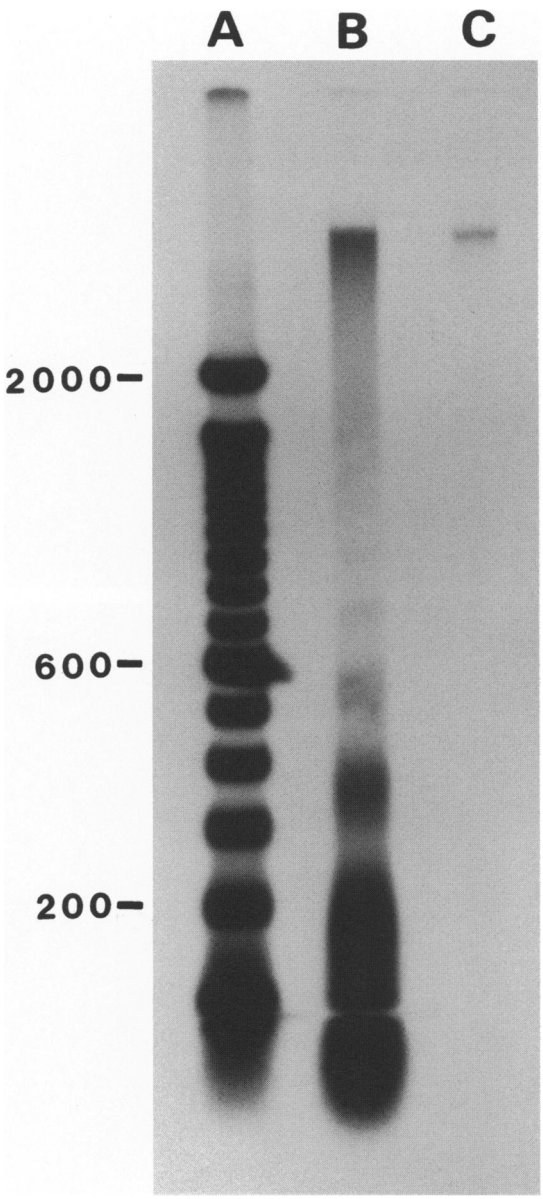

Figure 4. *The results of gel electrophoresis are shown.* **Lane A** *shows the radioactively labeled 100-bp DNA molecular weight markers. The 2000-bp, 600-bp, and 200-bp markers are illustrated.* **Lane B** *shows DNA extracted and purified from a PNET that exhibits cleavage of DNA at intervals of approximately 185 bp. The smearing of low molecular weight DNA species may reflect the presence of focal necrosis in this PNET in addition to apoptosis. No DNA fragmentation or smearing was seen in the control cerebellar DNA shown in* **lane C**.

the control cerebellum (Figure 4, lane C). The smearing of DNA in the PNETs probably reflects the presence of some coincidental necrosis.

The TUNEL labeling rate (Figure 3B) remained <0.5% in transgenic animals <10 weeks of age. Higher TUNEL labeling rates were seen only in transgenic mice >10 weeks old. Interestingly, the relationship between TUNEL labeling and age roughly paralleled the relationship between the BrdU labeling rate and age (Figure 3, A and B).

We also studied the relationship between the BrdU and TUNEL labeling rates in the PNETs (Figure 3C), and we observed a direct and linear correlation between cell proliferation and cell death. Remarkably, a low BrdU labeling rate was usually accompanied by a low TUNEL labeling rate whereas a high BrdU labeling rate was usually accompanied by a high TUNEL labeling rate.

We also analyzed the ratio of the TUNEL and BrdU labeling rates (T/B ratio) as a function of age in the PNETs. We observed a T/B ratio <0.6 in all but two mice. This suggests that cell proliferation exceeds cell death in these PNETs. The low T/B ratio and the progressive growth of PNETs in the rTH-Tag mice are consistent with the notion that these PNETs arise when cell proliferation exceeds cell death in SV40-Tag-positive cells of the neuroepithelium ventral to the median eminence. However, as the extent of BrdU labeling and TUNEL labeling does not measure the absolute rate of cell proliferation and cell death, the T/B ratio must be interpreted very cautiously. Indeed, the T/B ratio may be influenced by a number of factors, including the rate of elimination of apoptotic cells, the length of cell cycle, and the duration of S phase.

Immunohistochemistry of Nascent PNETs

In the rTH-Tag line of transgenic mice, SV40-Tag is expressed in the tumor cells as well as in many normal cells in other regions of the brain that never develop a tumor.[21,22] Although many SV40-Tag-positive cells are found throughout the CNS, they are seen more frequently in the white matter. No tumor formation is observed in any part of the brain except the median eminence. In the preneoplastic and neoplastic lesions of the median eminence, SV40-Tag is expressed in PNETs at all stages during progression. In addition, immunoreactive TH was found only focally in some microscopic tumors, and in many advanced tumors, only a small portion of the tumor cells expressed TH. Thus, there is no obvious linkage between the expression of SV40-Tag and TH.

We also analyzed the cell lineage of the nascent and advanced PNETs by immunohistochemistry and noted strong N-CAM staining in every microscopic PNET in the transgenic animals regardless of their age (Figure 5A). In some microscopic lesions in the younger transgenics, only focal staining was noted. However, diffuse and strong staining was demonstrated in advanced tumors. Synaptophysin was not

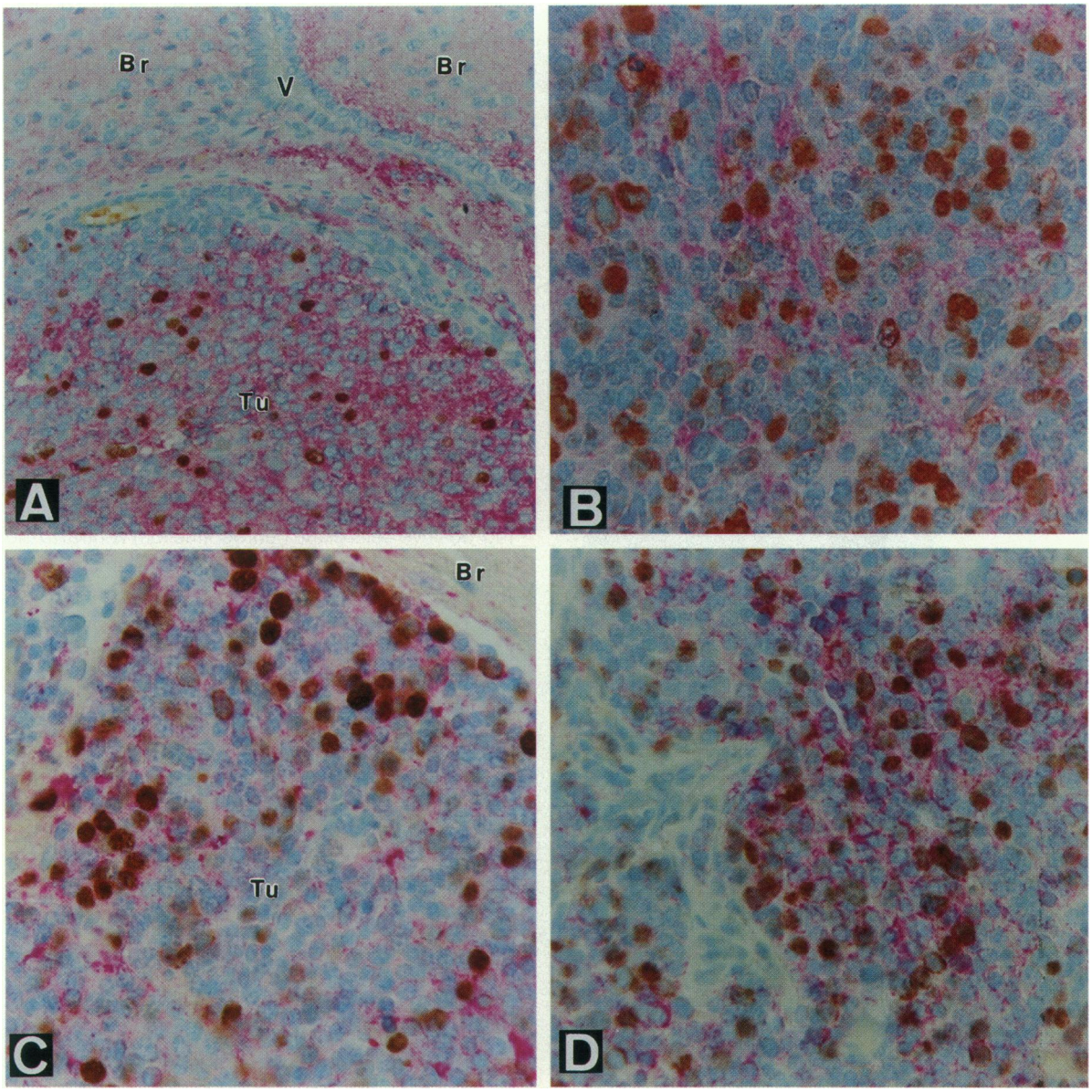

Figure 5. *Double immunostaining simultaneously demonstrates developmentally regulated proteins and BrdU incorporation in PNET cells. Positive nuclei in PNET cells are shown in brown in all figures, and the expression of N-CAM* (**A**)*, synaptophysin* (**B**)*, nestin* (**C**)*, and NF-L* (**D**) *are revealed in red in the same section. There is a higher level of N-CAM expression in the PNET relative to the adjacent brain* (**A**) *whereas N-CAM and synaptophysin are expressed diffusely in PNET cells regardless of their cell cycle status* (**A** *and* **B**, *respectively). Although nestin and NF-L* (**C** *and* **D**, *respectively) also are detected in cycling and noncycling PNET cells, they show a clonal expression pattern. V, distorted third ventricle; Br, non-neoplastic brain adjacent to the PNET; Tu, PNET.* (**A**, ×*250;* **B** *to* **D**, ×*500*)

expressed in the region of the ventral median eminence in the control animals, but it was expressed in both nascent and advanced PNETs (Figure 5B). In contrast, the expression of nestin and NF-L was weak and not consistently seen in every case in the early lesions, but in advanced tumors, nestin or NF-L were expressed strongly in a clonal pattern (Figure 5, C and D). Double staining by antibodies to both BrdU plus antibodies to either N-CAMs, synaptophysin, nestin, or NF-L revealed no consistent relationship between the cell cycle status of the PNET cells and the expression of these developmentally regulated antigens (Figure 5).

Discussion

In this study, we dissected the initial formation of experimental PNETs in mice carrying a SV40-Tag transgene. In the median eminence of rTH-Tag mice, we

observed PNETs arising from a group of neuroepithelial progenitor cells that failed to regress spontaneously as in their wild-type counterparts. After a latent period of approximately 10 weeks, an aberrant surge of sustained cell proliferation was observed in these cells that eventually led to the emergence of a PNET. Although cell death was detected consistently in these PNETs, the emergence of these PNETs implies that the rate of cell proliferation exceeded the rate of cell death. Thus, perturbation of the balance between cell proliferation and death as a result of a dramatic increase in proliferative activity may be the critical event that contributes to the induction and progression of these experimental PNETs. At the earliest stage in its formation (ie, 12th fetal day in mouse), the median eminence of both rats and mice appears as a group of densely packed cells approximately 6 to 10 layers thick lining the floor of the third ventricle.[42] As development proceeds, this layer of cells is separated from the third ventricle by the newly formed palisade zone, which is rich in dopaminergic axonal terminals. Although the precise embryonic origin of these neuroepithelial cells is not clearly known, these progenitor cells clearly regress and are replaced by capillaries of the primary portal plexus within the first 2 weeks of postnatal life as shown here and elsewhere[42,43] in the wild-type mice. However, in the rTH-Tag mice, this population of neuroepithelial cells does not regress, and the abrupt surge in cell proliferation in these cells in transgenic mice older than 10 weeks may reflect the occurrence of a second event that induces the formation of PNETs from pre-existing normal progenitor cells that express SV40-Tag.

As SV40-Tag is expressed at all stages in the evolution of these lesions, we conclude that SV40-Tag is necessary but not sufficient for tumor formation. The nature of this second event is uncertain, but it could represent the normal or aberrant expression of a trophic factor in this region. For example, recent studies of islet cell tumors in transgenic mice carrying SV40-Tag showed that the second event required for tumor induction was the expression of insulin-like growth factor-II (IGF-II) by islet cells and that IGF-II expression appeared to be necessary for tumor progression in SV40-Tag-expressing islet cells. In contrast, the islet cell tumors that developed in the absence of IGF-II remained small, had a high apoptotic rate, and progressed much slower compared with their counterparts in which IGF-II expression occurred.[46] In our study, we demonstrated SV40-Tag expression in the rTH-Tag mice at all stages in the emergence of PNETs. However, significant cell proliferation (as evidenced by BrdU labeling) was seen only in nascent PNETs in mice >10 weeks old. Thus, a latent period precedes the occurrence of a second event that confers a growth advantage to these nascent PNET cells, and it is possible that this second event varies in different types of CNS tumors or in different CNS regions. However, transgenic mouse models of tumors such as the one described here may be extremely useful experimental systems in which to identify factor(s) or event(s) that drive tumor progression.

In this study, we also demonstrated that cell death occurs in nascent and well established PNETs. Indeed, our findings suggest that apoptosis may be the major form of cell death in these experimental PNETs. As cell death (including apoptotic death) coexists with cell proliferation in spontaneous and experimental tumors,[5,6,45,47] including human medulloblastomas,[7] cell death may play a major role in regulating the induction and progression of CNS tumors of the immature brain. For example, spontaneous tumor regression has been observed in neural tumors such as malignant melanoma, retinoblastoma, and neuroblastoma.[48–50] Thus, apoptosis may be the major mechanism leading to regression in these tumors. In experimental tumors generated by xenografts of fibroblasts transfected with different oncogenes, apoptosis appears to be the critical factor in controlling the expansion rate of the tumor.[47] However, a high apoptotic rate also may occur in highly malignant tumors such as lymphomas[6] in which a high apoptotic rate may have little effect on malignant tumors with a very high cell proliferation rate.

Although the present study focused on the aberrant proliferation and cell death in the emergence of PNETs from progenitor cells in the neuroepithelium of the ventral median eminence, it is likely that an imbalance between cell proliferation and cell death in the developing brain could have other outcomes of pathological and behavioral significance. For example, they could lead to the under- or overpopulation of brain regions by neurons or glia. Indeed, SV40-Tag-expressing transgenic mice have been shown to result in the excess death of photoreceptor cells[26] and cerebellar Purkinje cells.[27] It is interesting to speculate whether or not more subtle phenotypes develop in such mice as a result of the excess production of neurons and glia that does not progress to tumor formation as in the rTH-Tag mice studied here. Nonetheless, we anticipate that the transgenic mice expressing SV40-Tag described here may provide an important model system for studies of the dynamic interplay between cell death and proliferation that results in divergent disease phenotypes such as tumors and malformations of the CNS.

Acknowledgments

Appreciation is expressed to Dr. D. M. Chikaraishi for early collaboration on this project and to Dr. L. B. Rorke for helpful comments on this manuscript. We are indebted to Drs. R. Mackay, G. Rougon, and J. Butel who kindly made antibodies available to us. We also thank Ms. S. Venkatachalam and Ms. J. M. Minda for their technical assistance. Statistical advice was kindly provided by Dr. I. Numah.

References

1. Kerr JFT, Wyllie AH, Currie AR: Apoptosis: a basic biological phenomenon with wide ranging implications in tissue kinetics. Br J Cancer 1972, 26:239–257
2. Wyllie AH: Apoptosis. Br J Cancer 1993, 67:205–208
3. Ferrer I, Bernet E, Soriano E, Del Rio T, Fonseca M: Naturally occurring cell death in the cerebral cortex of the rat and removal of dead cells by transitory phagocytes. Neuroscience 1990, 39:451–458
4. Budtz PE: Epidermal homeostasis: a new model that includes apoptosis. Apoptosis. II. The Molecular Basis of Apoptosis in Disease Edited by LD Tomei, FO Cope. Cold Spring Harbor, NY, Cold Spring Harbor Laboratory Press, 1994, pp 165–183
5. Fukasawa Y, Ishikura H, Takada A, Yokoyama S, Imamura M, Yoshiki T, Sato H: Massive apoptosis in infantile myofibromatosis: a putative mechanism of tumor regression. Am J Pathol 1994, 144:480–485
6. Leoncini L, Vecchio MTD, Hegha T, Barbini P, Galieni P, Pilen S, Sabattini E, Gherlinzoni F, Tosi P, Kraft R, Cottier H: Correlations between apoptotic and proliferative indices in malignant non-Hodgkin's lymphomas. Am J Pathol 1993, 142:755–763
7. Shiffer D, Cavalla P, Chiò A, Giordana MT, Marino S, Mauro A, Migheli A: Tumor cell proliferation and apoptosis in medulloblastoma. Acta Neuropathol 1994, 87: 362–370
8. Hermeking H, Eick D: Mediation of c-*myc*-induced apoptosis by p53. Science 1994, 265:2091–2093
9. Miura M, Zhu H, Rotello R, Hartwieg EA, Yuan J: Induction of apoptosis in fibroblasts by IL-1β-converting enzyme, a mammalian homolog of the *C. elegans* cell death gene *ced*-3. Cell 1993, 75:653–660
10. Tanaka N, Ishihiara M, Kitagawa M, Harada H, Kimura T, Matsuyama T, Lampher MS, Aizawa, Mark TW, Taniguchi T: Cellular commitment to oncogene-induced transformation or apoptosis is dependent on the transcription factor IRF-1. Cell 1994, 77:829–839
11. White K, Grether ME, Abrams JM, Young L, Farrel K, Steller H: Genetic control of programmed cell death in *Drosophila*. Science 1994, 264:677–683
12. Freeman RS, Estus S, Johnson EM: Analysis of cell-cycle related gene expression in postmitotic neurons: selective induction of cyclin D1 during programmed cell death. Neuron 1993, 12:343–355
13. Tilly JL, Hsueh AJW: Microscale autoradiographic method for the qualitative and quantitative analysis of apoptotic DNA fragmentation. J Cell Physiol 1993, 154:519–526
14. Gould VE, Jansson DS, Molenaar WM, Rorke LB, Trojanowski JQ, Lee VM-Y, Packer RJ, Franke WW: Primitive neuroectodermal tumors of the central nervous system: patterns of expression of neuroendocrine markers, and all classes of intermediate filament proteins. Lab Invest 1990, 62:498–509
15. Hart MN, Earle KM: Primitive neuroectodermal tumors of the brain in children. Cancer 1973, 32:890–897
16. Rorke LB: The cerebellar medulloblastoma and its relationship to primitive neuroectodermal tumors. J Neuropathol Exp Neurol 1983, 42:1–15
17. Rorke LB: Experimental production of primitive neuroectodermal tumors and its relevance to human neuro-oncology. Am J Pathol 1994, 144:444–448
18. Trojanowski JQ, Fung K-M, Rorke LB, Tohyama T, Yachnis AT, Lee VM-Y: *In vivo* and *in vitro* models of medulloblastomas and other primitive neuroectodermal brain tumors of childhood. Mol Chem Neuropathol 1994, 21:219–239
19. Molenaar WM, Jansson DS, Gould VE, Rorke LB, Franke WW, Lee VM-Y, Packer RJ, Trojanowski JQ: Molecular markers of primitive neuroectodermal tumors (PNETs) and other pediatric central nervous system tumors: monoclonal antibodies to neuronal and glial antigens distinguish subsets of PNETs. Lab Invest 1989, 61:635–643
20. Tohyama T, VM-Y Lee, Rorke LB, Marvin M, McKay RDG, Trojanowski JQ: Nestin expression in embryonic human neuroepithelium and in human neuroepithelial tumor cells. Lab Invest 1992, 66:301–313
21. Fung K-M, Chikaraishi DM, Theuring F, Messing A, Albert DM, Lee VM-Y, Trojanowski JQ: Molecular phenotype of Simian virus 40 large T antigen-induced primitive neuroectodermal tumors in four different lines of transgenic mice. Lab Invest 1994, 70: 114–124
22. Suri C, Fung BP, Tischler AS, Chikaraishi DM: Catecholaminergic cell lines from the brain and adrenal glands of tyrosine hydroxylase-SV40 T antigen transgenic mice. J Neurosci 1993, 13:1280–1291
23. Vogelstein B, Kinzler KW: The multistep nature of cancer. Trends Genet 1993, 9:138–141
24. Merlino G: Regulatory imbalances in cell proliferation and cell death during oncogenesis in transgenic mice. Semin Cancer Biol 1994, 5:13–20
25. Adams JM, Cory S: Transgenic models of tumor development. Science 1991, 254:1161–1167
26. Al-Ubaidi MR, Hollyfield JG, Overbeek PA, Baehr W: Photoreceptor degeneration induced by the expression of Simian virus 40 large tumor antigen in the retina of transgenic mice. Proc Natl Acad Sci USA 1992, 89:1194–1198
27. Fedderson RM, Ehlenfeldt R, Yunis WS, Clark HB, Orr HT: Disrupted cerebellar cortical development

and progressive degeneration of Purkinje cells in SV40 T antigen transgenic mice. Neuron 1992, 9:955–966
28. Hammang JP, Behringer RR, Baetge EE, Palmiter RD, Brinster RL, Messing A: Oncogene expression in retinal horizontal cells of transgenic mice results in a cascade of neurodegeneration. Neuron 1993, 10:1197–1209
29. Largent BL, Sosnowski RG, Reed RR: Directed expression of an oncogene to the olfactory neuronal lineage in transgenic mice. J Neurosci 1993, 13:300–312
30. Efrat S, Teitelman G, Anwar M, Ruggiero D, Hanahan D: Glucagon gene regulatory region directs oncoprotein expression to neurons and pancreatic cells. Neuron 1988, 1:605–613
31. Pan HC, Griep AE: Altered cell-cycle regulation in the lens of HPV-16 E6 or E7 transgenic mice: implication for tumor-suppressor gene function in development. Genes Dev 1994, 8:1285–1299
32. Nowakowski RS, Lewin SB, Miller MW: Bromodeoxyuridine immunohistochemical determination of the lengths of the cell cycle and the DNA-synthetic phase for an anatomically defined population. J Neurocytol 1989, 18:311–318
33. Gavrieli Y, Sherman Y, Ben-Sasson S: Identification of programmed cell death *in situ* via specific labeling of nuclear DNA fragmentation. J Cell Biol 1992, 119: 493–501
34. Brinster RL, Chen HY, Messing A, van Dyke T, Levine AJ, Palmiter RD: Transgenic mice harboring SV40-T antigen genes develop characteristic brain tumors. Cell 1984, 37:367–379
35. Gennarini G, Rougon G, Deagostini-Bazin H, Hirn M, Goridis C: Studies on the transmembrane disposition of the neutral cell adhesion molecule N-CAM. Eur J Biochem 1984, 142:57–64
36. Sepulveda AR, Finegold MJ, Smith B, Slagle BL, DeMayo JL, Shen RF, Woo SL, Butel JS: Development of a transgenic mouse system for the analysis of stages in liver carcinogenesis using tissue-specific expression of SV40 large T-antigen controlled by regulatory elements of the human-1-antitrypsin gene. Cancer Res 1989, 49:6108–6117
37. Wiedenmann B, Huttner WB: Synaptophysin and chromogranins/secretogranins: widespread constituents of distinct types of neuroendocrine vesicles and new tools in tumor diagnosis. Virchows Arch B Cell Pathol 1989, 58:95–121
38. Rohrer H, Acheson AL, Thibault J, Thoenen H: Developmental potential of quail dorsal root ganglion cells analyzed *in vitro* and *in vivo*. J Neurosci 1986, 6:2616–2624
39. Meyer J, Nauert J, Koehm S, Hughes J: Cell kinetics of human tumors by *in vitro* bromodeoxyuridine labeling. J Histochem Cytochem 1989, 37:1449–1454
40. Yachnis AT, Rorke LB, Lee VM-Y, Trojanowski JQ: Expression of neuronal and glial polypeptides during histogenesis of human cerebellar cortex including observations on the dentate nucleus. J Comp Neurol 1993, 334:356–369
41. Yachnis AT, Rorke LB, Trojanowski JQ: Cerebellar dysplasias in humans: development and possible relationship to glial and primitive neuroectodermal tumors of the cerebellar vermis. J Neuropathol Exp Neurol 1994, 53:61–71
42. Monroe BG, Paull WK: Ultrastructural changes in the hypothalamus during development and hypothalamic activity: the median eminence. Prog Brain Res 1974, 41:185–208
43. Ugrumov MV: Development of the median eminence during ontogenesis (morpho-functional aspects). Prog Brain Res 1992, 91:349–356
44. Jacobson M: The germinal cell, histogenesis, and lineages of nerve cells. Developmental Neurobiology, ed 3. New York, Plenum Press, 1994, p 46
45. Russel JH: Internal disintegration model of cytotoxic lymphocyte-induced target damage. Immunol Rev 1983, 72:97–118
46. Christofori G, Nalk P, Hanahan D: A second signal supplied by insulin-like growth factor II in oncogene-induced tumorigenesis. Nature 1994, 369:414–418
47. Arends MJ, McGregor AH, Wyllie AH: Apoptosis is inversely related to necrosis and determines net growth in tumors bearing constitutively expressed *myc*, *ras*, and HPV oncogenes. Am J Pathol 1994, 144:1045–1057
48. Boniuk M, Girard LJ: Spontaneous regression of bilateral retinoblastoma. Trans Am Acad Ophthalmol Otolaryngol 1969, 73:194–198
49. Carlsen NL: Neuroblastoma: epidemiology and pattern of regression: problems in interpreting results of mass screening. Am J Pediatr Hematol Oncol 1992, 14:103–110
50. Ceballos PI, Barnhill RL: Spontaneous regression of cutaneous tumors. Adv Dermatol 1993, 8:229–261